Cancer Science
Japanese Cancer Association JCA
Open Access

Y-632 inhibits heat shock protein 90 (Hsp90) function by disrupting the interaction between Hsp90 and Hsp70/Hsp90 organizing protein, and exerts antitumor activity *in vitro* and *in vivo*

Wenqian Wang,[1] Yang Liu,[1] Zhixin Zhao, Chengying Xie, Yongping Xu, Youhong Hu, Haitian Quan and Liguang Lou

Shanghai Institute of Materia Medica, Chinese Academy of Sciences, Shanghai, China

Key words
Hop, Hsp90, imatinib resistance, thiol oxidation, Y-632

Correspondence
Haitian Quan or Liguang Lou, Shanghai Institute of Materia Medica, Chinese Academy of Sciences, 555 Zuchongzhi Rd, Shanghai 201203, China.
Tel: +86-21-5080-6056; Fax: +86-21-5080-7088;
E-mails: haitianquan@simm.ac.cn (Haitian Quan); lglou@mail.shcnc.ac.cn (Liguang Lou)

Funding Information
National Natural Science Foundation of China (Y201181042, 81273546); Shanghai Science and Technology Committee (14DZ2294100); Ministry of Science and Technology of China, National Science and Technology Major Project "Key New Drug Creation and Manufacturing Program", China (2013ZX09102008, 2013ZX09402102-001).

[1]These authors contributed equally to this work.

Received January 18, 2016; Revised March 15, 2016; Accepted March 17, 2016

Cancer Sci **107** (2016) 782–790

doi: 10.1111/cas.12934

Heat shock protein 90 (Hsp90) stabilizes a variety of proteins required for cancer cell survival and has been identified as a promising drug target for cancer treatment. To date, several Hsp90 inhibitors have entered into clinical trials, but none has been approved for cancer therapy yet. Thus, exploring new Hsp90 inhibitors with novel mechanisms of action is urgent. In the present study, we show that Y-632, a novel pyrimidine derivative, inhibited Hsp90 in a different way from the conventional Hsp90 inhibitor geldanamycin. Y-632 induced degradation of diverse Hsp90 client proteins through the ubiquitin–proteasome pathway, as geldanamycin did; however, it neither directly bound to Hsp90 nor inhibited Hsp90 ATPase activity. Y-632 inhibited Hsp90 function mainly through inducing intracellular thiol oxidation, which led to disruption of the Hsp90–Hsp70/Hsp90 organizing protein complex and further induced cell adhesion inhibition, G_0/G_1 cell cycle arrest, and apoptosis. Moreover, Y-632 efficiently overcame imatinib resistance mediated by Bcr-Abl point mutations both *in vitro* and *in vivo*. We believe that Y-632, acting as a novel small-molecule inhibitor of the Hsp90–Hsp70/Hsp90 organizing protein complex, has great potential to be a promising Hsp90 inhibitor for cancer therapy, such as for imatinib-resistant leukemia.

Heat shock protein 90 is a ubiquitously expressed and highly conserved ATPase-dependent molecular chaperone. By forming a large multiprotein complex in cohort with diverse co-chaperones such as Hsp70, Cdc37, and Hop, Hsp90 plays an essential role in post-translational conformational maturation, stabilization, and activation of a broad range of client proteins, most of which are directly involved in tumor growth and survival.[1,2] Thus, inhibition of Hsp90 leads to degradation of these proteins and ultimately causes cancer cell growth arrest and apoptosis.[3] To date, several Hsp90 inhibitors have been under development and are being evaluated as a possible strategy for cancer treatment.[4,5]

In 1999, 17-AAG, a derivative of the first Hsp90 inhibitor GA, entered into clinical trials.[6] Since then, 16 distinct Hsp90 inhibitors, including natural product derivatives and fully synthetic small molecules, have been selected for clinical studies.[7–9] These compounds all bind to the N-terminal ATP/ADP binding site of Hsp90 and abolish its ATPase activity. Despite the fact that a few Hsp90 inhibitors are in clinical trials, none has been approved for cancer therapy.[10]

Based on high throughput drug screening, we have found a pyrimidine derivative, Y-632, to be a novel Hsp90 inhibitor with a structure distinct from current ones. In the present study, we show that Y-632 inhibited cell adhesion, caused cell cycle arrest, and apoptosis. Y-632 caused degradation of Hsp90 client proteins through inducing intracellular thiol oxidation and thus disrupted Hsp90–Hop interaction in an ATPase-independent mechanism. Moreover, Y-632 efficiently overcame imatinib resistance mediated by Bcr-Abl point mutations both *in vitro* and *in vivo*. Therefore, it is believed that Y-632 is a novel and promising Hsp90 inhibitor for cancer therapy.

Materials and Methods

Reagents and antibodies. Y-632 was synthesized at the Shanghai Institute of Materia Medica, Chinese Academy of

© 2016 The Authors. Cancer Science published by John Wiley & Sons Australia, Ltd on behalf of Japanese Cancer Association.
This is an open access article under the terms of the Creative Commons Attribution-NonCommercial-NoDerivs License, which permits use and distribution in any medium, provided the original work is properly cited, the use is non-commercial and no modifications or adaptations are made.

Sciences (Shanghai, China). Imatinib mesylate was obtained from Selleck Chemicals (Houston, TX, USA). Geldanamycin was obtained from Sangon Biotech (Shanghai, China). MG132, proteasome inhibitor I (PS341), chloroquine, MDL28170, monobromobimane, SRB, MTT, and antibodies against β-tubulin and insulin-like growth factor 1 receptor were purchased from Sigma-Aldrich (St. Louis, MO, USA). Antibodies against human epidermal growth factor receptor-2, GAPDH, EGFR, c-Met, Akt, phospho-Akt (Ser473), Cdk4, Cdk6, p85, poly-(ADP-ribose) polymerase, caspase 8, caspase 9, Hop, Cdc37, Erk1/2, and phospho-Erk1/2 (Thr202/Tyr204) were purchased from Cell Signaling Technology (Beverly, MA, USA). Antibodies against β-actin, Raf-1, p23, and caspase 3 were from Santa Cruz Biotechnology (Santa Cruz, CA, USA). Antibodies against Hsp90 and Bcr-Abl were from Abcam (Cambridge, UK). Anti-Hsp70 antibody was from Enzo Life Sciences (Farmingdale, NY, USA). Antiphosphotyrosine antibody (clone 4G10) was obtained from Millipore (Billerica, MA, USA).

Cell culture and treatment. Cell lines K-562, SK-BR-3, MCF7, A-431, and SNU-5 were obtained from ATCC (Manassas, VA, USA) and cultured according to instructions provided.

Western blot analysis and immunoprecipitation. Whole-cell lysates were prepared, separated by SDS-PAGE, and transferred to PVDF membranes. After incubation with primary and secondary antibody, immunoreactive proteins were detected using the enhanced chemiluminescence system from Thermo Fisher Scientific (Waltham, MA, USA).

For analysis of Triton-soluble and insoluble protein, Western blot was carried out essentially as described previously.[11] Briefly, cells were lysed in Triton X-100 lysis buffer (50 mM Tris-HCl, 150 mM NaCl, 1 mM EDTA, 1 mM EGTA, 1% Triton X-100, 20 μg/mL leupeptin, 2 mM sodium orthovanadate, 1 mM PMSF, 5 mM sodium fluoride, and 5000 U/mL aprotinin) and the lysates were centrifuged, then the supernatants were collected as Triton-soluble fraction and the pellet (Triton-insoluble fraction) was lysed with 2% SDS in 50 mM Tris-HCl then boiled for 15 min.

For immunoprecipitation, whole-cell lysates were incubated with anti-Hsp90 antibody and protein G agarose (Pierce, Rockford, IL, USA). Then the levels of immunoprecipitated proteins were analyzed by Western blot. Detailed procedures were referred to a previous report.[12]

Each photograph of Western blot analyses is from the same lysate and is representative of three separate experiments.

Colorimetric adhesion assay. The cell adhesion assay was carried out as described previously.[13] Drug-treated cells were added to 96-well plates that were precoated with 1% gelatin and incubated at 37°C for 3 h. Then detached cells were washed with PBS (pH 7.4) containing 0.05% Tween-20 and adhered cells were analyzed using SRB assay.

Cell cycle analysis. The cell cycle distribution was measured by propidium iodide staining, a typical method for cell cycle analysis since the 1970s.[14–19] Briefly, cells were fixed with ice-cold 70% ethanol overnight and stained with 50 μg/mL propidium iodide and 50 μg/mL RNase A.[20] The cell cycle was then measured by using a FACScan flow cytometer (BD Biosciences, San Jose, CA, USA) and analyzed with CellQuest Pro (BD Biosciences) and ModFit LT 3.0 software (Verity Software House).

Cell proliferation assay. Cells were incubated with various concentrations of drugs in 96-well plates and cultured for 72 h. Cell proliferation was determined by SRB assay for adherent cells or MTT assay for suspended cells as described previously.[20,21]

Colorimetric determination of ATPase activity. Inhibition of yeast Hsp90 ATPase activity was detected by malachite green assay.[22] In brief, 0.2 mg/mL yeast Hsp90 was incubated with drugs in assay buffer (100 mM Tris-HCl [pH 7.4], 20 mM KCl, and 6 mM $MgCl_2$) containing 1 mM ATP (Sigma-Aldrich). After incubation at 37°C for 4 h, malachite green reagent was added, followed by the injection of 34% sodium citrate. The mixture was then incubated for 15 min at room temperature and the absorbance at 620 nm was measured using a Synergy H4 Hybrid reader (BioTek, Winooski, VT, USA).

Surface plasmon resonance analysis. In general, SPR was carried out as described previously.[23] First, the CM5 sensor chip was balanced with running buffer (10 mM HEPES [pH 7.4], 0.15 M KCl, and 0.001% Tween-20) for 10 min at 25°C to prevent non-specific binding of proteins to the capillaries of the Biacore 3000 (GE Healthcare, Cleveland, OH, USA) instrument. Then human recombinant Hsp90α (150 μg/mL in 10 mM sodium acetate [pH 4.3]) was immobilized on the CM5 chip surface. Non-covalently bound Hsp90 was quenched with 1 M ethanolamine. Compounds were injected from lowest to highest concentrations at a flow rate of 30 μL/min. An additional 3 min was needed to monitor the dissociation of the compound–protein complex.

Luciferase refolding assay. Luciferase refolding assay was carried out as described previously.[24] Rabbit reticulocyte lysate (Promega, Madison, WI, USA) was incubated with DMSO (control) or drugs for 30 min at 37°C. Firefly luciferase (Sigma-Aldrich) was denatured for 10 min at 41°C and refolding reaction was initiated after drug-pretreated RRL was injected. The reaction system was incubated at 25°C for 2 h and then the luciferase activity was detected.

Detection of intracellular free thiol levels. Monobromobimane was used to determine intracellular free thiol levels.[25] After drug treatment, cells were collected, plated into 96-well plates, and then loaded with 100 μM monobromobimane for 30 min in the dark. The fluorescence was detected with excitation and emission wavelengths at 390 and 460 nm, respectively.

***In vivo* study.** All animal experiments were carried out in accordance with the Institutional Animal Care and Use Committee guidelines at the Shanghai Institute of Materia Medica, Chinese Academy of Sciences. Female nude mice (Balb/cA-nude, 5–6 weeks old) were purchased from Shanghai SLAC Laboratory Animal Co., Ltd (Shanghai, China). Cells (32D-WT or 32D-T315I, 10×10^7) were implanted s.c. into nude mice. After 48 h of inoculation, mice were randomized into four groups with 7–11 mice each group. The animal number required in each group was based on a comprehensive review of published reports[26,27] and the 3R (reduction, refinement, and replacement) principles of the Institutional Animal Care and Use Committee guidelines at the Shanghai Institute of Materia Medica, Chinese Academy of Sciences. Mice were then treated with vehicle (60% PEG-400, i.p.), Y-632 (7 mg/kg/day and 10 mg/kg/day, i.p.), or imatinib mesylate (200 mg/kg/day, p.o.) for a total of 16 days. Tumor volume was calculated as $width^2 \times length \times 0.5$ and body weight was monitored as an indicator of general health.

For the pharmacodynamics study, mice bearing tumors received a single i.p. of 10 mg/kg Y-632 or vehicle and then tumor tissues were collected at 8 h post-dosing. Tumor samples were homogenized in RIPA buffer and analyzed by Western blot.

© 2016 The Authors. Cancer Science published by John Wiley & Sons Australia, Ltd on behalf of Japanese Cancer Association.

Statistical analysis. Results of repetitive experiments are presented as mean ± SD or mean ± SEM. A two-tailed Student's *t*-test was used for comparison of treatment *versus* control groups. Statistical analysis was carried out using GraphPad Prism 6 software (GraphPad Software, Inc., San Diego, CA, USA).

Results

Y-632 induces degradation of diverse Hsp90 client proteins through ubiquitin–proteasome pathway. In searching for novel Hsp90 inhibitors, a panel of pyrimidine derivatives was rationally designed from the structure–activity relationships investigation and structure optimization based on a hit compound Y-498 (Fig. 1a), which has been identified as an Hsp90 inhibitor. The derivatives were screened, based on their effects on Hsp90 client proteins and Hsp70 level, and Y-632 was ultimately identified (Fig. 1a). In Bcr-Abl-overexpressing leukemia K-562 cells, Y-632 reduced different Hsp90 client proteins levels (Bcr-Abl, Raf-1, Akt, and Cdk6) in a time- and dose-dependent manner (Fig. 1b). Correspondingly, extensive elevation of Hsp70 was observed (Fig. 1b). Y-632 also induced diverse Hsp90 client protein degradation and Hsp70 elevation in SK-BR-3, A-431, MCF7 and SNU-5 cells, which overexpress human epidermal growth factor receptor-2, EGFR, insulin-like growth factor 1 receptor, and c-Met, respectively (Fig. 1c). Moreover, the protein level of non-Hsp90-dependent protein p85 was not altered. As a positive Hsp90 inhibitor, GA also significantly decreased Hsp90 client proteins and induced Hsp70 expression (Fig. 1b,c).

Most Hsp90 inhibitors induce misfolded protein degradation through the ubiquitin–proteasome pathway.[28] Once proteins

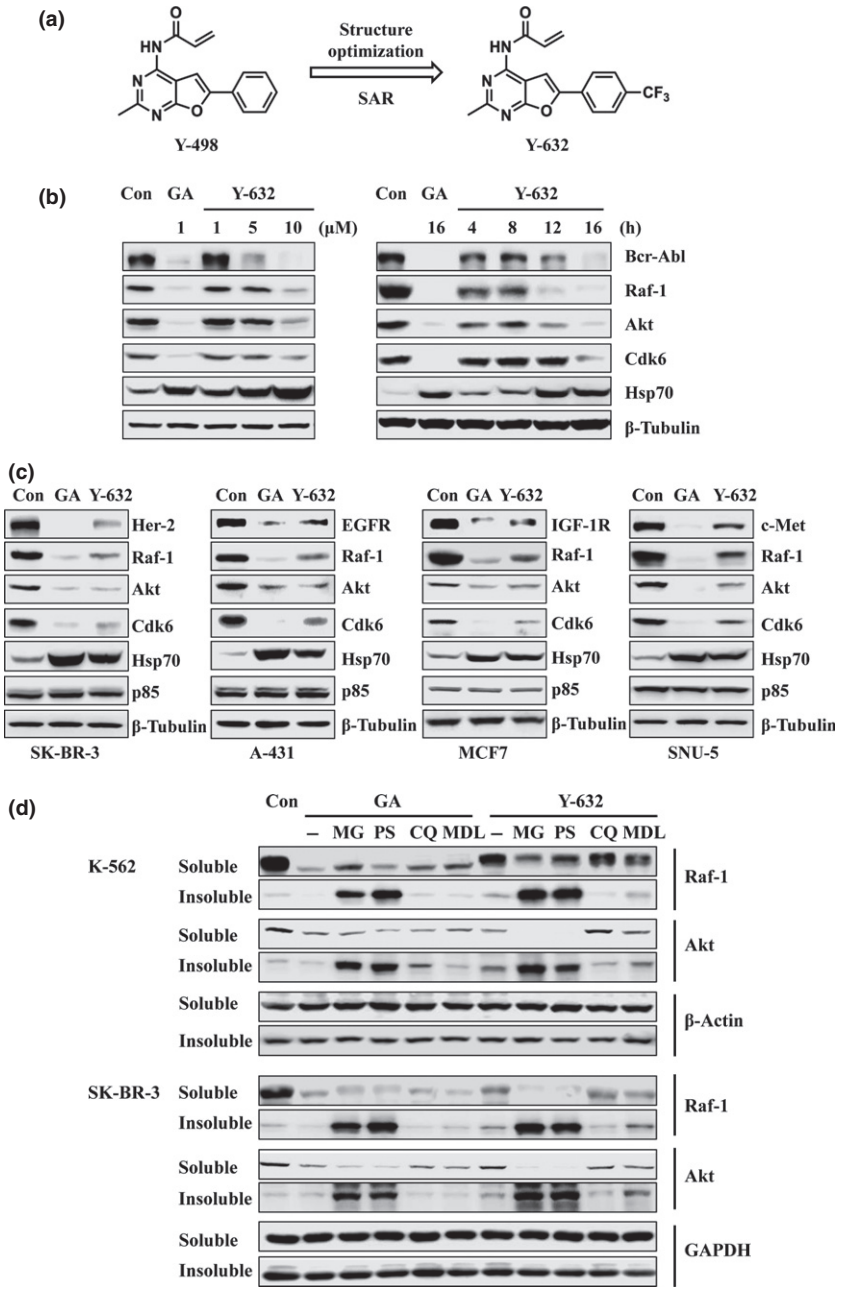

Fig. 1. Y-632 induces heat shock protein 90 (Hsp90) client protein degradation through the ubiquitin–proteasome pathway. (a) Chemical structure of Y-632, a derivative of Y-498. SAR, structure–activity relationship. (b) K-562 cells were exposed to DMSO (Con), geldanamycin (GA; 1 μM, 16 h), or Y-632 at indicated periods or concentrations and analyzed by Western blot. (c) Cells were treated with 1 μM GA or 10 μM Y-632 for 16 h and analyzed by Western blot. (d) Cells were pretreated with proteasome inhibitor PS341 (PS; 1 μM) or MG132 (MG; 10 μM), autophagy/lysosome inhibitor chloroquine (CQ; 50 μM), or calpain inhibitor MDL28170 (MDL; 50 μM) for 1 h, and then treated with GA (1 μM) or Y-632 (10 μM) for 16 h. Soluble fraction was prepared in lysis buffer containing 0.1% Triton X-100 and the insoluble fraction was prepared in 50 mM Tris-HCl containing 2% SDS. Protein levels were detected by Western blot. –, untreated; Akt, protein kinase B; Cdk6, cyclin-dependent kinase 6; Her-2, human epidermal growth factor receptor-2.

© 2016 The Authors. Cancer Science published by John Wiley & Sons Australia, Ltd on behalf of Japanese Cancer Association.

are misfolded and aggregated, their solubility will decrease. Being an appropriate detergent to distinguish proteins according to their solubility properties, Triton X-100 was used to increase the sensitivity of detection of proteins with low solubility.[29,30] As shown in Figure 1(d), the combination of Y-632 with proteasome inhibitors MG132[31] or PS341[32] induced significant elevation of ubiquitinated Raf-1 and Akt (insoluble fraction) both in K-562 and SK-BR-3 cells. In contrast, neither lysosome inhibitor chloroquine[33] nor calpain inhibitor MDL28170[34] mimicked the same effect, indicating that Y-632 triggered degradation in a ubiquitin–proteasome-dependent manner. Taken together, Y-632 showed the same effect as Hsp90 inhibitor GA did, raising the possibility that it may be a potential Hsp90 inhibitor.

Y-632 induces cell adhesion inhibition, G_0/G_1 cell cycle arrest, and cell apoptosis. We next assessed the biological effects of Y-632 *in vitro*. The observation that SK-BR-3 cells became round within 8 h after 10 μM Y-632 treatment (data not shown) suggested that Y-632 may affect cell adhesion. As expected, after treatment with 2.5 μM Y-632, adhesion rates of SK-BR-3 and A-431 cells were significantly reduced to 65.6% ($P < 0.01$) and 14.9% ($P < 0.0001$) of control, respectively, whereas the equal effect was not observed with GA even up to 10 μM (Fig. 2a), indicating that Y-632 potently inhibits tumor cell adhesion, in contrast to GA.

Then we detected the effect of Y-632 on the cell cycle and cell apoptosis. Twenty-four hours of Y-632 treatment induced G_0/G_1 cell cycle arrest in a dose-dependent manner in SK-BR-3, K-562, and A-431 cells, whereas GA arrested cells at G_2 phase (Fig. 2b), as reported previously.[35] Furthermore, cell apoptosis was induced by prolonged Y-632 treatment (48 h), which was manifested by the concentration-dependent increase of cleaved caspase 8, decrease of procaspase 9 and procaspase 3, and cleavage of poly-(ADP-ribose) polymerase (Fig. 2c).

Y-632 inhibits Hsp90 function by disturbing Hsp90–Hop interaction rather than inhibiting Hsp90 ATPase activity. Next, the specific mechanism of Y-632 was explored. To investigate whether Y-632 inhibited Hsp90 ATPase activity, we undertook a malachite green assay using recombinant full-length yeast Hsp90. Considering the IC_{50} values of Hsp90 inhibitors for Hsp90 ATPase activity are reported to be much higher than the concentrations that could induce degradation of Hsp90

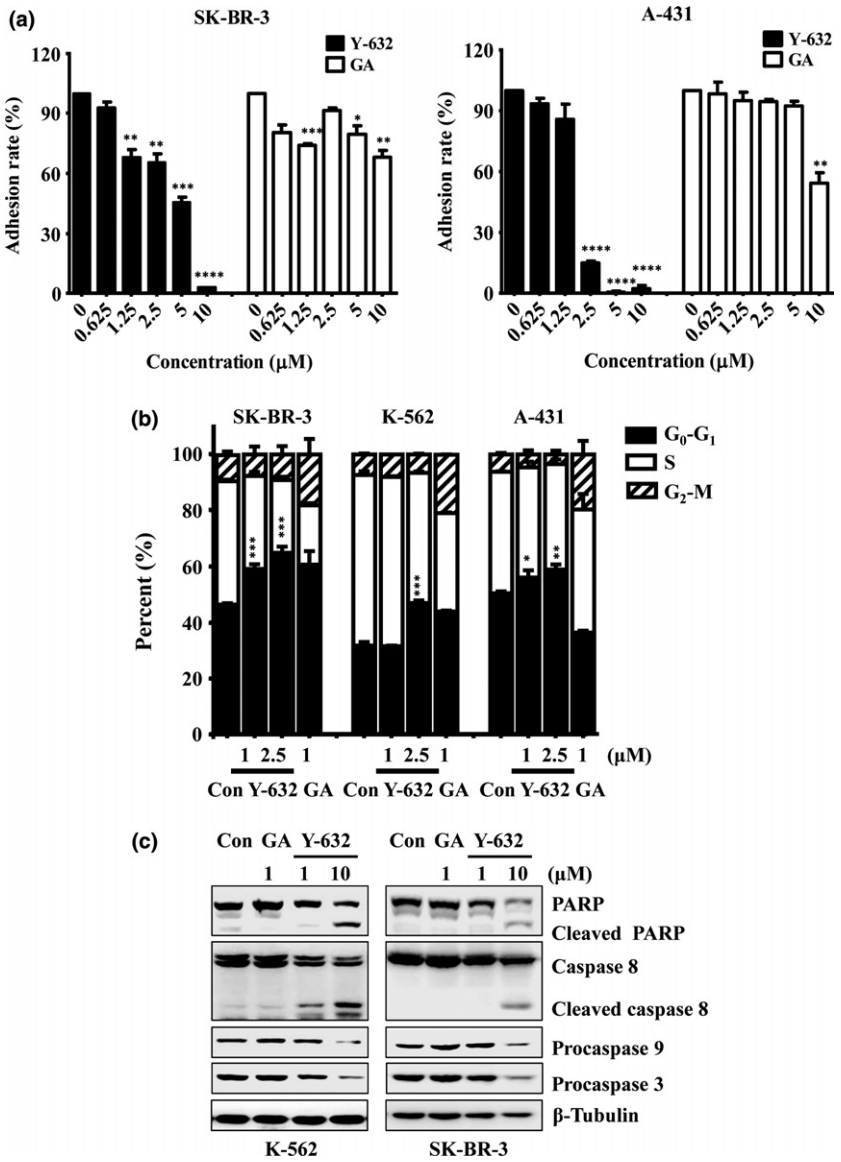

Fig. 2. Y-632 induces cell adhesion inhibition, G_0/G_1 cell cycle arrest, and cell apoptosis in cancer cells. (a) After treated with indicated concentrations of geldanamycin (GA) or Y-632 for 30 min, cells were plated into 96-well plates and cell adhesion was determined. (b) After 24 h of treatment with Y-632 or GA, cells were collected and analyzed by flow cytometry. (c) Cells were exposed to indicated concentrations of GA or Y-632 for 48 h and analyzed by Western blot. Results in (a,b) are shown as mean ± SD of at least three independent experiments. $^*P < 0.05$; $^{**}P < 0.01$; $^{***}P < 0.001$; $^{****}P < 0.0001$. PARP, poly-(ADP-ribose) polymerase.

© 2016 The Authors. Cancer Science published by John Wiley & Sons Australia, Ltd on behalf of Japanese Cancer Association.

client proteins in tumor cells,[36–38] the concentration of Y-632 we used in this assay was up to 500 μM. As shown in Figure 3(a), GA significantly abolished Hsp90 ATPase activity by 49% ($P < 0.05$) and 95% ($P < 0.001$) at 1 μM and 100 μM, respectively, but Y-632 had no significant effect on Hsp90 ATPase activity. Next, we used SPR assay to assess the affinity

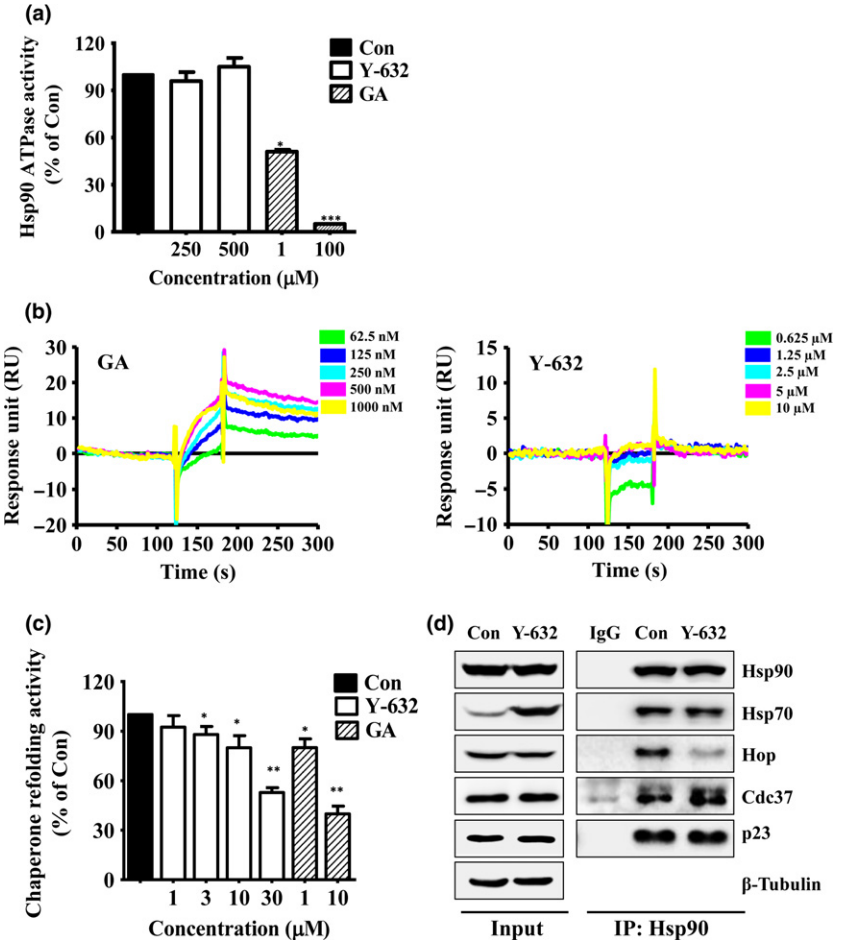

Fig. 3. Y-632 inhibits heat shock protein 90 (Hsp90) complex by disturbing Hsp90–Hsp70/Hsp90 organizing protein (Hop) interaction rather than inhibiting Hsp90 ATPase activity. (a) ATPase activity of yeast Hsp90 was determined by malachite green assay. (b) Surface plasmon resonance analysis of Y-632 binding to full-length Hsp90α. Sensor grams obtained by injection of Y-632 and geldanamycin (GA) at the indicated concentrations on immobilized Hsp90α. (c) Denatured luciferase was refolded in DMSO- or drug-treated rabbit reticulocyte lysate and the activity of luciferase was measured by luciferase refolding assay. (d) After treated with 10 μM Y-632 for 16 h, K-562 cells were immunoprecipitated (IP) with Hsp90 antibody and levels of Hop or other Hsp90 co-chaperones were detected by Western blot. Results in (a,c) are shown as mean ± SD of at least three independent experiments. *$P < 0.05$; **$P < 0.01$; ***$P < 0.001$; ****$P < 0.0001$.

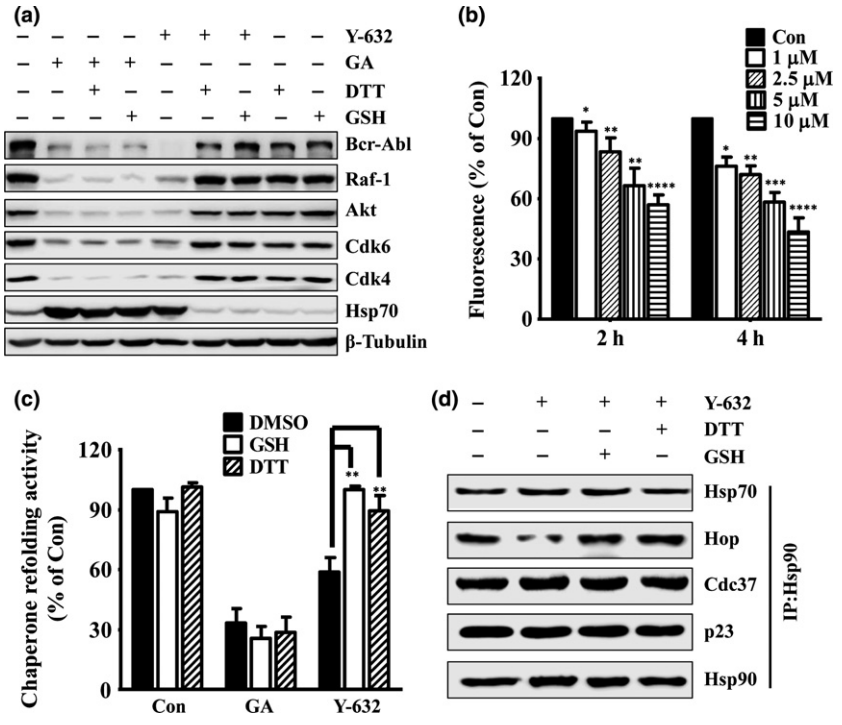

Fig. 4. Y-632 inhibits heat shock protein 90 (Hsp90) chaperone through decreasing intracellular thiol levels. (a) After incubation with 10 μM DTT or 10 μM glutathione (GSH) at 37°C for 1 h, 1 μM geldanamycin (GA) or 10 μM Y-632 was used to treat K-562 cells for another 12 h. Then cells were collected and analyzed by Western blot. (b) After the indicated treatment with Y-632, K-562 cells were loaded with monobromobimane and fluorescence intensity was detected. (c) After pretreatment with 10 μM DTT or 10 μM GSH at 37°C for 1 h, 1 μM GA or 10 μM Y-632 was incubated with rabbit reticulocyte lysate at 37°C for 30 min. Luciferase activity was detected as described earlier. (d) After treatment described in (a), K-562 cells were immunoprecipitated (IP) with Hsp90 antibody and levels of Hsp70/Hsp90 organizing protein (Hop) or other Hsp90 co-chaperones were detected by Western blot. Results in (b,c) are shown as mean ± SD of at least three independent experiments. *$P < 0.05$; **$P < 0.01$; ***$P < 0.001$; ****$P < 0.0001$. Akt, protein kinase B; Cdk, cyclin-dependent kinase; Con, control.

© 2016 The Authors. Cancer Science published by John Wiley & Sons Australia, Ltd on behalf of Japanese Cancer Association.

of Y-632 to purified recombinant human full-length Hsp90α. In contrast to GA, Y-632 showed no interaction with Hsp90 even up to 10 μM (Fig. 3b), indicating that Y-632 neither inhibits Hsp90 ATPase activity nor binds to Hsp90. Thus, we wondered whether Y-632 inhibited Hsp90 by damaging the super-chaperone complex machinery. Luciferase refolding assay was used to examine the effect of Y-632 on the ability of RRL, which is abundant in Hsp90 and its co-chaperones, to refold thermally denatured firefly luciferase. As shown in Figure 3(c), when treated with increasing concentrations of GA or Y-632, RRL showed reduced capability of refolding denatured luciferase to its native state, whereas the native luciferase activity was

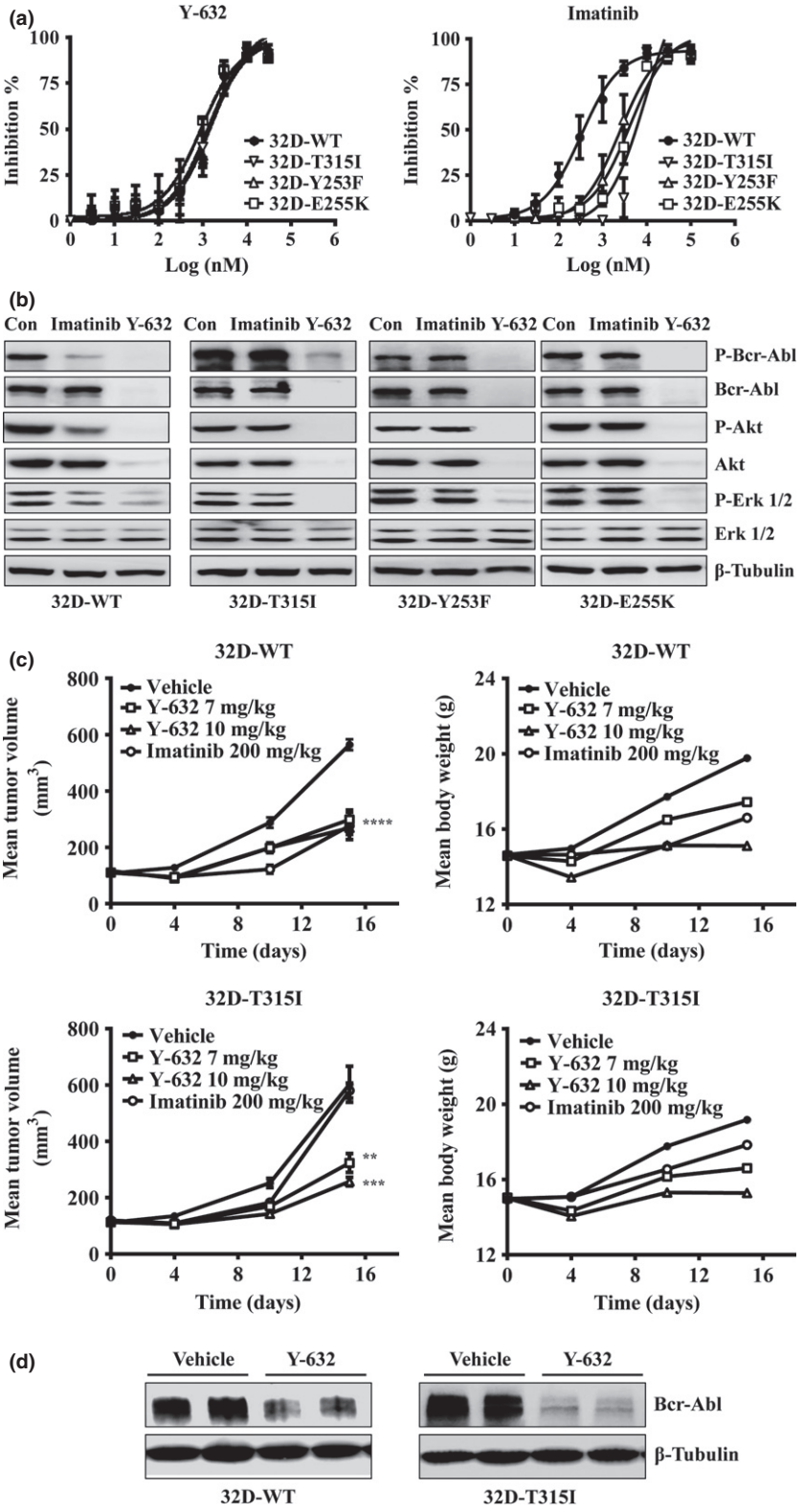

Fig. 5. Y-632 inhibits growth of imatinib-resistant cells both *in vitro* and *in vivo*. (a) Cell viability was measured by MTT assay after drug treatment. Results are shown as mean ± SD of at least three independent experiments. (b) Indicated cells were exposed to 0.3 μM imatinib for 3 h or 10 μM Y-632 for 12 h and analyzed by Western blot. (c) Nude mice bearing 32D/Bcr-Abl wild-type (32D-WT) or 32D-T315I (32D/Bcr-Abl T315I) xenograft tumors were treated with vehicle, indicated concentrations of Y-632, or imatinib daily for 16 days. Tumor volume was measured on the indicated days. Results are shown as mean ± SEM (vehicle group, $n = 11$; treatment groups, $n = 7$). (d) Mice were killed 8 h after the last dose and tumors were removed and analyzed by Western blot. $^{**}P < 0.01$; $^{***}P < 0.001$; $^{****}P < 0.0001$. Akt, protein kinase B; Con, control.

© 2016 The Authors. Cancer Science published by John Wiley & Sons Australia, Ltd on behalf of Japanese Cancer Association.

unaffected (data not shown), suggesting that Y-632 inhibits the Hsp90 super-chaperone complex. Next, we used immunoprecipitation assay to clarify which co-chaperone was involved. Significant downregulation of Hop was observed in 16 h Y-632-treated K-562 cells, while the total Hop protein level was unchanged. Other co-chaperones such as Hsp70, Cdc37, and p23 were not affected (Fig. 3d). Thus, it was indicated that Y-632 inhibits Hsp90 mainly by disturbing the interaction of Hsp90 and Hop.

Y-632 reduces intracellular thiol levels and thus leads to Hsp90 inhibition. Recently, researchers have reported that post-transcriptional modifications of Hsp90 such as phosphorylation and oxidation have multiple impacts on Hsp90 function.[39,40] In addition, thiol-reactive small molecules can modify Hsp90's cysteine residues and further affect its function both *in vitro* and *in vivo*.[41,42] With a thiol-reactive α, β-unsaturated bond structure, Y-632-induced Hsp90 complex oxidation was considered to be a possible mechanism of action. As shown in Figure 4(a), when pre-incubated with thiol-containing antioxidants GSH or DTT, both Y632-induced Hsp90 client proteins (Bcr-Abl, Raf-1, Akt, Cdk4, Cdk6) degradation and Hsp70 elevation were reversed, suggesting that Y-632 probably inhibits Hsp90 through thiol oxidation. Next, we tested the intracellular thiol state after Y-632 treatment using monobromobimane, a reagent that forms fluorescent adducts after conjugated with thiol-containing molecules. Indeed, Y-632 significantly decreased thiol levels in K-562 cells in a time- and dose-dependent manner. Four hours of treatment with 10 μM Y-632 resulted in almost 50% ($P < 0.0001$) decrease of total thiol levels (Fig. 4b). Moreover, GSH and DTT both restored Y-632's inhibition of reticulocyte lysate to refold denatured luciferase, but not GA's (Fig. 4c). The effect Y-632 on Hsp90–Hop interaction was also reversed by GSH and DTT (Fig. 4d). These results indicate that Y-632 induces thiol oxidation, leading to Hsp90–Hop complex disruption and further Hsp90 inhibition.

Y-632 inhibits growth of imatinib-resistant cells both *in vitro* and *in vivo*. Imatinib resistance is a major impediment in chronic myelogenous leukemia therapy, and acquisition of point mutations in the kinase domain of Bcr-Abl is the major mechanism.[43] As Y-632 could induce Bcr-Abl degradation, we wondered whether it could overcome imatinib resistance induced by certain Bcr-Abl mutants. As shown in Figure 5(a), imatinib inhibited the proliferation of 32D cells harboring wild-type Bcr-Abl (32D-WT), but had a much weaker effect on other cells expressing transforming Bcr-Abl mutants. In contrast, Y-632 showed nearly equivalent IC_{50} values towards 32D cells bearing wild-type or mutant Bcr-Abl. Consistent with these results, Y-632 induced the degradation of Bcr-Abl, leading to phosphorylation inhibition of Bcr-Abl and downstream Akt and Erk1/2 in both 32D cell lines (Fig. 5b).

The *in vitro* potential of Y-632 to overcome imatinib resistance prompted us to investigate its effect *in vivo*. T315I is the most resistant mutant of Bcr-Abl,[43] thus, we studied the *in vivo* efficacy of Y-632 in 32D-T315I xenografts. Y-632 (10 mg/kg/day) potently inhibited the growth of both 32D-WT and 32D-T315I tumors by 66.6% ($P < 0.0001$) and 77.1% ($P < 0.001$), respectively, whereas imatinib (200 mg/kg/day) had an inhibitory effect (63.6%, $P < 0.0001$) only on 32D-WT xenografts (Fig. 5c). To further investigate whether Y-632-induced tumor growth inhibition was related to its effect on Bcr-Abl, we measured Bcr-Abl protein level in tumor tissues. As shown in Figure 5(d), Y-632 reduced the expression of Bcr-Abl in both 32D-WT and 32D-T315I tumors. Taken together, these results indicate that Y-632 efficiently overcomes imatinib resistance induced by Bcr-Abl point mutations, such as the T315I mutation, both *in vitro* and *in vivo*.

Discussion

In this study, we investigated the antitumor activity and mechanisms of Y-632. Unlike the classical Hsp90 inhibitors, Y-632 neither directly bound to Hsp90 nor inhibited Hsp90 ATPase activity. Instead, it significantly induced thiol oxidation, thus disrupted Hsp90–Hop interaction and inhibited Hsp90 function. In addition, Y-632 potently overcame imatinib resistance both *in vitro* and *in vivo*. We believe that Y-632, as a novel Hsp90 inhibitor, has great potential to be further investigated.

Most Hsp90 inhibitors inhibit Hsp90 function by regulating its ATPase activity.[44] In recent years, increased efforts have focused on Hsp90 post-translational modifications, such as oxidation, which provide alternative ways for Hsp90 inhibition.[45,46] Tubocapsenolide A, a novel withanolide, induces a decrease of intracellular thiol levels, causes direct thiol oxidation of Hsp90, triggers Hsp90 to form intermolecular disulfide bonds, and consequently leads to Hsp90 client protein degradation.[11] Mahanine, a carbazole alkaloid, induces thiol oxidation and disulfide linkage of Hsp90, leading to the disruption of Hsp90–Cdc37 interaction.[47] In this study, we showed that Y-632 also inhibited Hsp90 through thiol oxidation. However, the exact mechanism was different from those reported previously, as Y-632 inhibited Hsp90 mainly by disrupting Hsp90–Hop interaction. Why the same thiol oxidation results in diverse mechanisms of Hsp90 inhibition is not yet clear. As cellular oxidative metabolism is complex, it is likely that these compounds have distinct thiol-reactive groups, and different thiol-reactive groups may have distinct affinities towards diverse intracellular reductive groups, which may lead to oxidation of different molecules in cells and thus result in diverse mechanisms of Hsp90 inhibition. However, the specific mechanism needs to be further investigated.

Heat shock protein 90 requires diverse co-chaperones to form a super-chaperone complex for its function.[48] Therefore, targeting the interaction of Hsp90 and its co-chaperones may be an alternative way to achieve the outcomes of direct Hsp90 inhibition.[49] One exciting finding in our study is that Y-632 disrupts Hsp90–Hop interaction; Hop is one of the Hsp90 co-chaperones and plays an essential role in transfecting unfolded polypeptide from Hsp70 to Hsp90.[50] In metastatic or drug-resistant tumors such as breast, ovarian, and colon carcinomas, Hop is upregulated, indicating that it is associated with cancer biology.[51,52] To date, only a few agents have been discovered to disrupt Hsp90–Hop interaction. C9, a small molecule identified by an AlphaScreen technology, disrupts Hsp90–Hop interaction by binding to the TPR2A domain of Hop.[53,54] Our report shows that Y-632 disrupted Hsp90–Hop interaction through thiol oxidation, which is quite different from C9. Considering susceptible cysteine residues are largely located at the Hsp90 C-terminal, which has the binding site of Hop,[42,55] we speculate that Y-632 may induce oxidation of these cysteine residues and finally interfere with the interaction of Hop and Hsp90. Further study is still warranted to find the exact mechanism.

Point mutations in kinases such as Bcr-Abl, c-Kit, and EGFR lead to kinase inhibitor resistance, which is a major obstacle of cancer therapy.[43,56,57] Y-632 could inhibit the growth of imatinib-resistant cells both *in vitro* and *in vivo*, indicating Y-632 might have clinical application in overriding drug resistance caused by mutated oncoproteins, such as

© 2016 The Authors. Cancer Science published by John Wiley & Sons Australia, Ltd on behalf of Japanese Cancer Association.

Bcr-Abl T315I. In addition, considering the mechanism of Y-632 on Hsp90 inhibition was distinct from the conventional Hsp90 inhibitors, we suggest that the combination of Y-632 with conventional Hsp90 inhibitors might result in better antitumor efficacy, which may broaden Y-632's application. However, for better understanding of Y-632's pharmacological effect, the effects of Y-632 on normal hematopoietic cells need to be further investigated.

In conclusion, Y-632 disrupts Hsp90–Hop interaction, causes degradation of Hsp90 client proteins by inducing intracellular thiol oxidation, and exerts antitumor activity *in vitro* and *in vivo*. It is especially efficient at overcoming drug resistance caused by mutated oncoproteins, such as Bcr-Abl T315I. It is believed that Y-632 is a promising Hsp90 inhibitor with a novel mechanism, and has great potential to be further developed.

Acknowledgments

This work was supported by research funding from the National Natural Science Foundation of China (Grant Nos. Y201181042 and 81273546), the Shanghai Science and Technology Committee (Grant No. 14DZ2294100), and the National Science and Technology Major Project "Key New Drug Creation and Manufacturing Program", China (Grant Nos. 2013ZX09102008 and 2013ZX09402102-001).

Disclosure Statement

The authors have no conflict of interest.

Abbreviations

Akt	protein kinase B
Cdc37	cell division cycle 37
Cdk	cyclin-dependant kinase
32D-T315I	32D/Bcr-Abl T315I cells
32D-WT	32D/Bcr-Abl wild-type cells
EGFR	epidermal growth factor receptor
GA	geldanamycin
GSH	glutathione
Hop	Hsp70/Hsp90 organizing protein
Hsp	heat shock protein
RRL	rabbit reticulocyte lysate
SPR	surface plasmon resonance
SRB	sulforhodamine B

References

1 Whitesell L, Lindquist SL. HSP90 and the chaperoning of cancer. *Nat Rev Cancer* 2005; **5**: 761–72.
2 Trepel J, Mollapour M, Giaccone G, Neckers L. Targeting the dynamic HSP90 complex in cancer. *Nat Rev Cancer* 2010; **10**: 537–49.
3 Hostein I, Robertson D, DiStefano F, Workman P, Clarke PA. Inhibition of signal transduction by the Hsp90 inhibitor 17-allylamino-17-demethoxygeldanamycin results in cytostasis and apoptosis. *Cancer Res* 2001; **61**: 4003–9.
4 Hong DS, Banerji U, Tavana B, George GC, Aaron J, Kurzrock R. Targeting the molecular chaperone heat shock protein 90 (HSP90): lessons learned and future directions. *Cancer Treat Rev* 2013; **39**: 375–87.
5 Tatokoro M, Koga F, Yoshida S, Kihara K. Heat shock protein 90 targeting therapy: state of the art and future perspective. *EXCLI J* 2015; **14**: 48–58.
6 Sausville EA, Tomaszewski JE, Ivy P. Clinical development of 17-allylamino, 17-demethoxygeldanamycin. *Curr Cancer Drug Targets* 2003; **3**: 377–83.
7 Sidera K, Patsavoudi E. HSP90 inhibitors: current development and potential in cancer therapy. *Recent Pat Anticancer Drug Discov* 2014; **9**: 1–20.
8 Kim T, Keum G, Pae AN. Discovery and development of heat shock protein 90 inhibitors as anticancer agents: a review of patented potent geldanamycin derivatives. *Expert Opin Ther Pat* 2013; **23**: 919–43.
9 Taldone T, Gozman A, Maharaj R, Chiosis G. Targeting Hsp90: small-molecule inhibitors and their clinical development. *Curr Opin Pharmacol* 2008; **8**: 370–4.
10 Bhat R, Tummalapalli SR, Rotella DP. Progress in the discovery and development of heat shock protein 90 (Hsp90) inhibitors. *J Med Chem* 2014; **57**: 8718–28.
11 Chen WY, Chang FR, Huang ZY, Chen JH, Wu YC, Wu CC. Tubocapsenolide A, a novel withanolide, inhibits proliferation and induces apoptosis in MDA-MB-231 cells by thiol oxidation of heat shock proteins. *J Biol Chem* 2008; **283**: 17184–93.
12 Wang Q, Quan H, Zhao J, Xie C, Wang L, Lou L. RON confers lapatinib resistance in HER2-positive breast cancer cells. *Cancer Lett* 2013; **340**: 43–50.
13 Zong H, Wang F, Fan QX, Wang LX. Curcumin inhibits metastatic progression of breast cancer cell through suppression of urokinase-type plasminogen activator by NF-kappa B signaling pathways. *Mol Biol Rep* 2012; **39**: 4803–8.
14 Krishan A. Rapid flow cytofluorometric analysis of mammalian cell cycle by propidium iodide staining. *J Cell Biol* 1975; **66**: 188–93.
15 Xu C, Fu H, Gao L *et al.* BCR-ABL/GATA1/miR-138 mini circuitry contributes to the leukemogenesis of chronic myeloid leukemia. *Oncogene* 2014; **33**: 44–54.
16 Yu C, Yu C, Krystal G *et al.* Pharmacologic mitogen-activated protein/extracellular signal-regulated kinase kinase/mitogen-activated protein kinase inhibitors interact synergistically with STI571 to induce apoptosis in Bcr/Abl-expressing human leukemia cells. *Cancer Res* 2002; **62**: 188–99.
17 Ahmad N, Feyes DK, Agarwal R, Mukhtar H. Photodynamic therapy results in induction of WAF1/CIP1/P21 leading to cell cycle arrest and apoptosis. *Proc Natl Acad Sci U S A* 1998; **95**: 6977–82.
18 Kumar R, Mendelsohn J. Role of 2'-5'-oligoadenylate synthetase in gamma-interferon-mediated growth inhibition of A431 cells. *Cancer Res* 1989; **49**: 5180–4.
19 Lee JH, Jung KH, Lee H *et al.* HS-133, a novel fluorescent phosphatidylinositol 3-kinase inhibitor as a potential imaging and anticancer agent for targeted therapy. *Oncotarget* 2014; **5**: 10180–97.
20 Quan H, Liu H, Li C, Lou L. 1,4-Diamino-2,3-dicyano-1,4-bis(methylthio) butadiene (U0126) enhances the cytotoxicity of combretastatin A4 independently of mitogen-activated protein kinase kinase. *J Pharmacol Exp Ther* 2009; **330**: 326–33.
21 Zhao J, Quan H, Xu Y, Kong X, Jin L, Lou L. Flumatinib, a selective inhibitor of BCR-ABL/PDGFR/KIT, effectively overcomes drug resistance of certain KIT mutants. *Cancer Sci* 2014; **105**: 117–25.
22 Rowlands MG, Newbatt YM, Prodromou C, Pearl LH, Workman P, Aherne W. High-throughput screening assay for inhibitors of heat-shock protein 90 ATPase activity. *Anal Biochem* 2004; **327**: 176–83.
23 Horibe T, Kohno M, Haramoto M, Ohara K, Kawakami K. Designed hybrid TPR peptide targeting Hsp90 as a novel anticancer agent. *J Transl Med* 2011; **9**: 8.
24 Galam L, Hadden MK, Ma Z *et al.* High-throughput assay for the identification of Hsp90 inhibitors based on Hsp90-dependent refolding of firefly luciferase. *Bioorg Med Chem* 2007; **15**: 1939–46.
25 Chen WY, Wu CC, Lan YH, Chang FR, Teng CM, Wu YC. Goniothalamin induces cell cycle-specific apoptosis by modulating the redox status in MDA-MB-231 cells. *Eur J Pharmacol* 2005; **522**: 20–9.
26 Bright SA, McElligott AM, O'Connell JW *et al.* Novel pyrrolo-1,5-benzoxazepine compounds display significant activity against resistant chronic myeloid leukaemia cells in vitro, in ex vivo patient samples and in vivo. *Br J Cancer* 2010; **102**: 1474–82.
27 Shi X, Chen X, Li X *et al.* Gambogic acid induces apoptosis in imatinib-resistant chronic myeloid leukemia cells via inducing proteasome inhibition and caspase-dependent Bcr-Abl downregulation. *Clin Cancer Res* 2014; **20**: 151–63.
28 Mimnaugh EG, Chavany C, Neckers L. Polyubiquitination and proteasomal degradation of the p185c-erbB-2 receptor protein-tyrosine kinase induced by geldanamycin. *J Biol Chem* 1996; **271**: 22796–801.
29 Petrucelli L, Dickson D, Kehoe K *et al.* CHIP and Hsp70 regulate tau ubiquitination, degradation and aggregation. *Hum Mol Genet* 2004; **13**: 703–14.
30 Babu JR, Geetha T, Wooten MW. Sequestosome 1/p62 shuttles polyubiquitinated tau for proteasomal degradation. *J Neurochem* 2005; **94**: 192–203.
31 Figueiredo-Pereira ME, Berg KA, Wilk S. A new inhibitor of the chymotrypsin-like activity of the multicatalytic proteinase complex (20S proteasome) induces accumulation of ubiquitin-protein conjugates in a neuronal cell. *J Neurochem* 1994; **63**: 1578–81.

© 2016 The Authors. Cancer Science published by John Wiley & Sons Australia, Ltd on behalf of Japanese Cancer Association.

32 Rock KL, Gramm C, Rothstein L *et al.* Inhibitors of the proteasome block the degradation of most cell proteins and the generation of peptides presented on MHC class I molecules. *Cell* 1994; **78**: 761–71.
33 de Duve C. Lysosomes revisited. *Eur J Biochem* 1983; **137**: 391–7.
34 Song DK, Malmstrom T, Kater SB, Mykles DL. Calpain inhibitors block Ca (2+)-induced suppression of neurite outgrowth in isolated hippocampal pyramidal neurons. *J Neurosci Res* 1994; **39**: 474–81.
35 Kim HR, Lee CH, Choi YH, Kang HS, Kim HD. Geldanamycin induces cell cycle arrest in K562 erythroleukemic cells. *IUBMB Life* 1999; **48**: 425–8.
36 Cheung KM, Matthews TP, James K *et al.* The identification, synthesis, protein crystal structure and in vitro biochemical evaluation of a new 3,4-diarylpyrazole class of Hsp90 inhibitors. *Bioorg Med Chem Lett* 2005; **15**: 3338–43.
37 Huang W, Ye M, Zhang LR *et al.* FW-04-806 inhibits proliferation and induces apoptosis in human breast cancer cells by binding to N-terminus of Hsp90 and disrupting Hsp90-Cdc37 complex formation. *Mol Cancer* 2014; **13**: 150.
38 Nariai Y, Mizuguchi H, Ogasawara T *et al.* Disruption of Heat Shock Protein 90 (Hsp90)-Protein Kinase Cdelta (PKCdelta) Interaction by (-)-Maackiain Suppresses Histamine H1 Receptor Gene Transcription in HeLa Cells. *J Biol Chem* 2015; **290**: 27393–402.
39 Scroggins BT, Neckers L. Post-translational modification of heat-shock protein 90: impact on chaperone function. *Expert Opin Drug Discov* 2007; **2**: 1403–14.
40 Walton-Diaz A, Khan S, Bourboulia D, Trepel JB, Neckers L, Mollapour M. Contributions of co-chaperones and post-translational modifications towards Hsp90 drug sensitivity. *Future Med Chem* 2013; **5**: 1059–71.
41 Carbone DL, Doorn JA, Kiebler Z, Ickes BR, Petersen DR. Modification of heat shock protein 90 by 4-hydroxynonenal in a rat model of chronic alcoholic liver disease. *J Pharmacol Exp Ther* 2005; **315**: 8–15.
42 Martinez-Ruiz A, Villanueva L, Gonzalez de Orduna C *et al.* S-nitrosylation of Hsp90 promotes the inhibition of its ATPase and endothelial nitric oxide synthase regulatory activities. *Proc Natl Acad Sci U S A* 2005; **102**: 8525–30.
43 Shah NP, Sawyers CL. Mechanisms of resistance to STI571 in Philadelphia chromosome-associated leukemias. *Oncogene* 2003; **22**: 7389–95.
44 Jhaveri K, Taldone T, Modi S, Chiosis G. Advances in the clinical development of heat shock protein 90 (Hsp90) inhibitors in cancers. *Biochim Biophys Acta* 2012; **1823**: 742–55.
45 Alarcon SV, Mollapour M, Lee MJ *et al.* Tumor-intrinsic and tumor-extrinsic factors impacting hsp90- targeted therapy. *Curr Mol Med* 2012; **12**: 1125–41.
46 Mollapour M, Neckers L. Post-translational modifications of Hsp90 and their contributions to chaperone regulation. *Biochim Biophys Acta* 2012; **1823**: 648–55.
47 Sarkar S, Dutta D, Samanta SK *et al.* Oxidative inhibition of Hsp90 disrupts the super-chaperone complex and attenuates pancreatic adenocarcinoma in vitro and in vivo. *Int J Cancer* 2013; **132**: 695–706.
48 Workman P. Altered states: selectively drugging the Hsp90 cancer chaperone. *Trends Mol Med* 2004; **10**: 47–51.
49 Seo YH. Small Molecule Inhibitors to Disrupt Protein-protein Interactions of Heat Shock Protein 90 Chaperone Machinery. *J Cancer Prev* 2015; **20**: 5–11.
50 Schmid AB, Lagleder S, Grawert MA *et al.* The architecture of functional modules in the Hsp90 co-chaperone Sti1/Hop. *EMBO J* 2012; **31**: 1506–17.
51 Sims JD, McCready J, Jay DG. Extracellular heat shock protein (Hsp)70 and Hsp90alpha assist in matrix metalloproteinase-2 activation and breast cancer cell migration and invasion. *PLoS ONE* 2011; **6**: e18848.
52 Wang TH, Chao A, Tsai CL *et al.* Stress-induced phosphoprotein 1 as a secreted biomarker for human ovarian cancer promotes cancer cell proliferation. *Mol Cell Proteomics* 2010; **9**: 1873–84.
53 Yi F, Regan L. A novel class of small molecule inhibitors of Hsp90. *ACS Chem Biol* 2008; **3**: 645–54.
54 Pimienta G, Herbert KM, Regan L. A compound that inhibits the HOP-Hsp90 complex formation and has unique killing effects in breast cancer cell lines. *Mol Pharm* 2011; **8**: 2252–61.
55 Nardai G, Sass B, Eber J, Orosz G, Csermely P. Reactive cysteines of the 90-kDa heat shock protein, Hsp90. *Arch Biochem Biophys* 2000; **384**: 59–67.
56 Kobayashi S, Boggon TJ, Dayaram T *et al.* EGFR mutation and resistance of non-small-cell lung cancer to gefitinib. *N Engl J Med* 2005; **352**: 786–92.
57 Debiec-Rychter M, Sciot R, Le Cesne A *et al.* KIT mutations and dose selection for imatinib in patients with advanced gastrointestinal stromal tumours. *Eur J Cancer* 2006; **42**: 1093–103.

© 2016 The Authors. Cancer Science published by John Wiley & Sons Australia, Ltd on behalf of Japanese Cancer Association.